Paper # D09 Report LBNL-62505 **Topic: Fundamentals**

5^{th} US Combustion Meeting
Organized by the Western States Section of the Combustion Institute
and Hosted by the University of California at San Diego
March 25-28, 2007.

Diagnostics for the Combustion Science Workbench

J. F. Grcar, M. S. Day, and J. B. Bell

Center for Computational Science and Engineering
Lawrence Berkeley National Laboratory
1 Cyclotron Road
Berkeley, California 94720-8142, USA

As the cost of computers declines relative to outfitting and maintaining laser spectroscopy laboratories, computers will account for an increasing proportion of the research conducted in fundamental combustion science. W. C. Gardiner foresaw that progress will be limited by the ability to understand the implications of what has been computed and to draw inferences about the elementary components of the combustion models. Yet the diagnostics that are routinely applied to computer experiments have changed little from the sensitivity analyses included with the original CHEMKIN software distribution. This paper describes some diagnostics capabilities that may be found on the virtual combustion science workbench of the future. These diagnostics are illustrated by some new results concerning which of the hydrogen/oxygen chain branching reactions actually occur in flames, the increased formation of NOx in wrinkled flames versus flat flames, and the adequacy of theoretical predictions of the effects of stretch. Several areas are identified where work is needed, including the areas of combustion chemistry and laser diagnostics, to make the virtual laboratory a reality.

1 Introduction

Scientific research has always involved a combination of theory and experiment — and since the invention of the computer — simulation. Prominent contributors to early Combustion Symposia, [1], were among the first to use computers once the machines became available for civilian scientific research in the early 1950s. Computer simulations held the promise to reveal the many minor species that were hypothesized to exist inside flames. Chemically and spatially detailed simulations were not feasible until some thirty years later, in the early 1980s [2], when adaptive mesh methods were applied to the steady-state equations for 1D, so-called flat, flames. Such simulations were widely distributed with the CHEMKIN software, [3], and finally afforded fairly complete models of laminar flames, [4]. Comparisons between these models and experiment remain the chief method of validating complete chemical mechanisms against actual flames, [5].

In the twenty-five years since 1D flame simulations were developed, research in computational methods for partial differential equations, [6, 7], has made it possible to simulate the temporal history of entire, laboratory-scale 2D laminar flames, [8, 9], and 3D turbulent flames, [10, 11]. Unlike traditional direct numerical simulations (DNS), the new methods use adaptive mesh refinement (AMR) and the low-Mach number formulation of the Navier Stokes equations to dramatically reduce the computational effort. These advanced mathematical methods and the ever increasing speed of computers now allow modest parallel computers of 16 processors to simulate 2D laminar

flames, while parallel computers of 128 processors may be capable of some 3D turbulent simulations. Moreover, unlike Reynolds-averaged (RANS) and large-eddy (LES) simulations, the new methods introduce no flamelet or turbulence models. Consequently, they can be used to study directly the fundamental relationships between fluid dynamics and flame chemistry.

These opportunities increase the difficulties of interpreting and communicating simulation results since W. C. Gardiner first described them in 1977 [12]:

> Chemists interested in computer modeling are no longer limited by the constraints of computation. Instead, progress in achieving understanding of the reactions under study is limited by the ability to understand the implications of what has been computed and to draw inferences about the elementary reactions comprising the reaction mechanism. After completion of a modeling study, it is also a serious communication problem to convey the essential results — and the justifications for the conclusions drawn — to other modeling experts or to the scientific community.

New methods of analysis and presentation may be needed beyond the traditional simulation diagnostics for flat flames: sensitivity analysis, reaction path analyses, line and 2D plots of species concentrations, and scatter plots of probability density functions. Some new approaches are: (1) computational singular perturbations [13–15] which is related to principal component analysis, (2) stochastic particles [16] which is a random walk approximation to a Markov process representing the kinetics, and (3) pathline analysis [17] which traces the changes to an "infinitesimally small" parcel of the fluid as it passes through the flame.

2 A Virtual Laboratory for Combustion Fundamentals

This paper illustrates some fundamental flame simulations and diagnostics that can be performed on them with modest computational resources. Please contact the authors for information about the availability of this software for research purposes.

Two freely propagating premixed laminar flames are considered: a hydrogen-air flame with (fuel) equivalence ratio $\phi = 0.5$, and a methane-air flame with $\phi = 0.6$. The pressure of the gas is 1 (atm) and the temperature of the unburned gas is 300 (K). The computational domains are 2D with toroidal (reentrant) boundary conditions at the left and right. The simulations begin with a randomly wrinkled flame zone extending from left to right across their respective domains. Unburned gas flows in from the bottom and burned gas flows out the top. The inflow is dynamically adjusted to steady the flames roughly midway between the inflow and outflow boundaries using the control algorithm described in [18].

Both simulations were performed using the algorithm of Day and Bell [8] which as noted employs adaptive mesh refinement (AMR) and the low-Mach number formulation of the flow equations. The GRI-Mech 3.0 chemical mechanism [5] is used for both flames, however, species and reactions involving carbon are removed for the hydrogen-air flame. A 16 processor parallel computer needed approximately one to two weeks of continuous calculation for each flame.

3 Premixed Hydrogen Flame

3.1 Instabilities

It is well known that freely propagating premixed hydrogen flames are both spatially and temporally unstable. *That is — in marked contrast to 1D simulations — the flames in nature are not flat.* For further discussion and experimental images see [19]. The spatial instability is manifest in cellular structures; the temporal instability is exhibited in a continual process of birth and death of the cells. Figure 1 displays the instability in two images of the simulated flame zone. The cellular structures at B and D in the upper frame extinguish because the adjacent cells are slightly upstream and therefore compete more successfully for fuel in the unburned gas. The cells at A, C, and E are creating new cells literally by cell division.

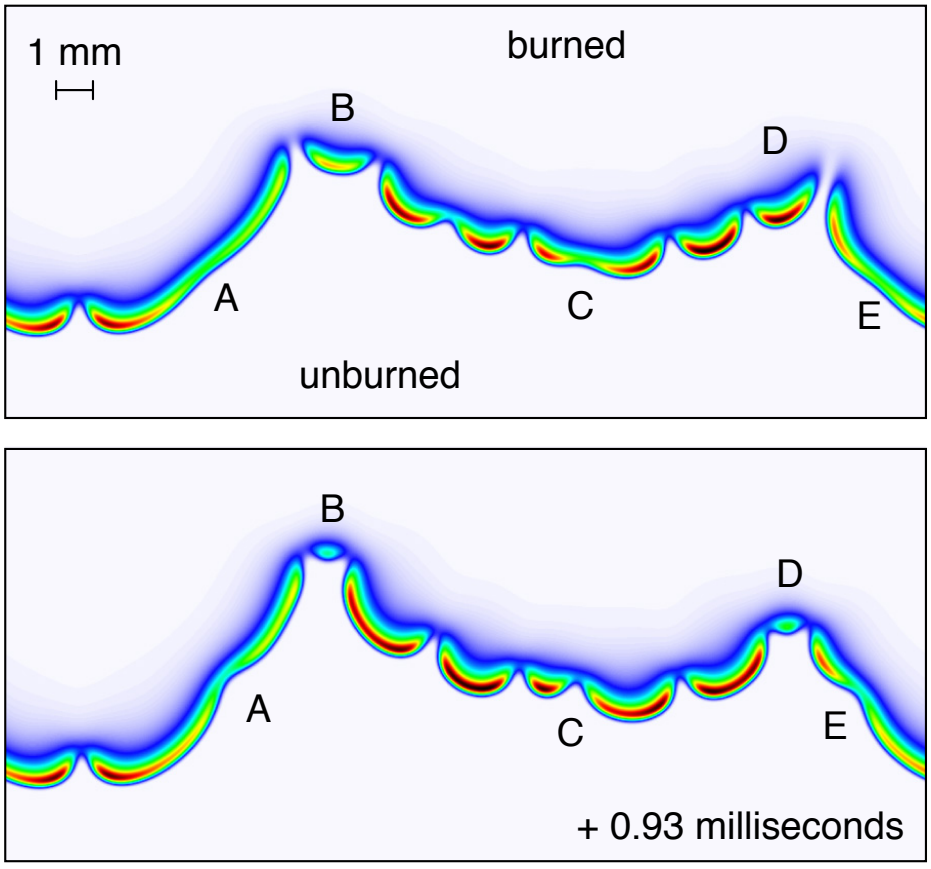

Figure 1: The freely propagating premixed hydrogen-air flame ($\phi = 0.5$) at two instants in time: earlier (above) and later (below). Pictured is the mole fraction of atomic hydrogen, $\mathrm{X(H)}$, in a linear rainbow scale from 0.0 (white) to 0.0069 (black).

3.2 Cellular Preference

The preference for cellular structures and the process of cell division can be understood through the joint distribution of temperature and fuel in the flame zone. Figure 2 depicts this distribution

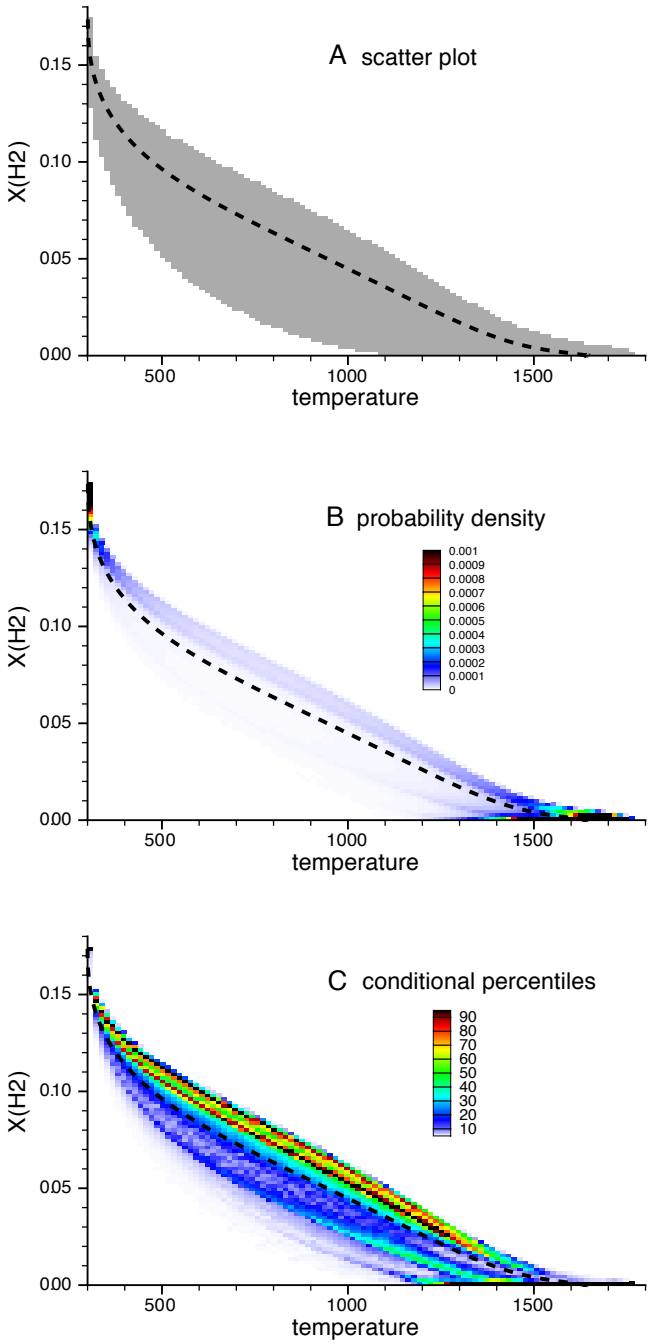

Figure 2: Joint distribution of fuel and temperature in the premixed hydrogen flame depicted three ways. In each plot the dashed line is the distribution for a flat laminar premixed flame calculated by the CHEMKIN software PREMIX [3].

three ways. In Figure 2A a simple scatter plot is shown. The distribution in the 2D flame (grey) clearly is more varied than in the 1D flame (dashed line), but apart from this little information is conveyed. In Figure 2B the joint probability density is plotted. The highest densities are those outside the flame zone consisting of unburned gas at the upper left in the figure, and burned gas at

the lower right. Since the flame itself occupies only a small portion of the computational domain, the probability density for any of the intermediate temperature is vanishingly small and barely discernible in the figure.

In Figure 2C the data displayed to greatest advantage after two simple transformations. First, the joint density is conditioned by position on the horizontal axis. That is, each vertical slice through the figure is a separate probability density for $\mathrm{X}(\mathrm{H}_2)$ at the given temperature, or in other words, the densities on each vertical slice have been scaled so the integral over the vertical line is 1.0. This has the effect of bringing out the details at the intermediate temperatures where the fame zone occurs independent of the rather of low probability density of the states in the flame zone. Second, rather than plot density, Figure 2C shows actual probability in terms of percentiles of the probability distribution. The color scale marks the percentiles in order from lowest density (white and blue) to highest (read and black). The method of displaying joint probabilities, which does not seem to appear in the statistical literature, is here called *conditional percentiles*. It is immediately clear from this approach, in Figure 2C, that the deciles colored turquoise and green through red and black lie above the dashed line corresponding to the laminar flame. This means that at each temperature in the flame zone, approximately 70% of the fuel exists at a higher mole fraction than would be found in the laminar flat flame.

Thus, Figure 2C shows that the bowed shape of the cellular structures increase the fuel in the flame zone to a level consistent with a mixture above the nominal equivalence ratio of $\phi = 0.5$. This richer mixture evidently gives the bowed cells an advantage in speed of propagation over the flat flame. Indeed, where the cells flatten — as at points A, C, and E in Figure 1 — the flame falls behind its more quickly advancing flanks. At these points the flame eventually extinguishes as the flames on either side rob it of fuel due to diffusion of hydrogen toward the points where it is most rapidly consumed. In previous work [19] it was found that the trailing spaces between the cells become completely depleted of fuel.

3.3 Hydrogen-Oxygen Chaining Reactions

Reaction path analysis is customarily used to account for the exchange of material among species in a chemically reacting system. A fairly complete analysis of this simulation diagnostic has recently been given elsewhere [20].

Here, reaction path diagrams are extended two ways to provide greater information about the underlying reaction mechanism. The diagrams customarily consist of chemical species connected by arrows that represent the transfer of atoms of one kind, usually carbon, from one species to another as a result of chemical reactions. The arrows may be annotated to indicate the responsible reaction(s). First, it is proposed to include the reactions themselves as nodes in the path diagram. This approach ties together the exchanges among multiple pairs of species that might be caused by a single reaction, thereby possibly highlighting a reaction's multiple functions. Second, it is proposed to include exchanges of atoms of several elements each represented by a distinctive color. This approach reveals to what extent the various reactions participate in transforming fuel or oxidizer or both to final products. Graphs of this kind will be called *reaction network diagrams*.

It is particularly revealing to depict the hydrogen-oxygen chain branching system in terms of a

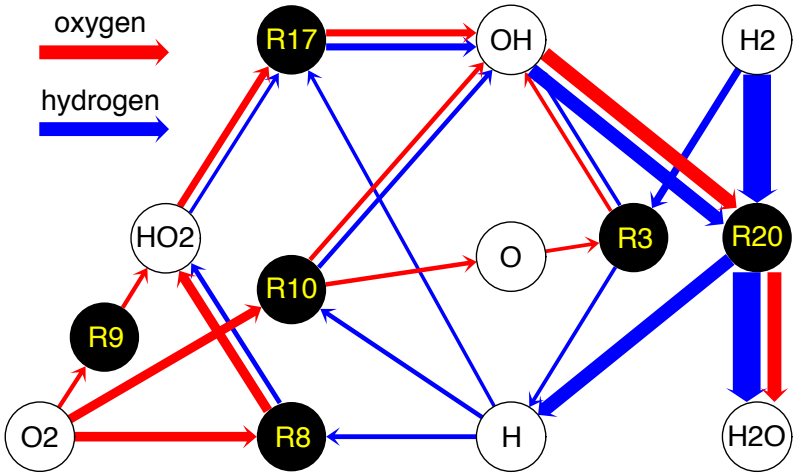

Figure 3: Reaction network diagram for the hydrogen-air flame simulation. Each arrow represents the integral over the computational domain of the rate of hydrogen or oxygen atoms moved among species by reactions occurring in the flame (final units mol / sec). The rate is proportional to the thickness of the arrow. For simplicity only paths at least 10% of the thickest are drawn. Table 1 identifies the reactions.

reaction network diagram. Figure 3 shows the diagram for the hydrogen-air flame, and Table 1 identifies the reactions. It is clear from the figure that reaction 20 simultaneously accounts for the bulk of the fuel consumed as well as for the creation of the final product. Notice that the path $\mathrm{OH} \rightarrow \mathrm{R20}$ limits the rate of the overall reaction because, presumably, OH is less abundant than the primary fuel. Moreover, hydrogen atoms lost in the path $\mathrm{R20} \rightarrow \mathrm{H}$ are entirely returned to the reaction through the path $\mathrm{OH} \rightarrow \mathrm{R20}$ after participating in breaking down the molecular oxygen through several paths. Thus by itself R20 can account for only a steady conversion of fuel to product. The reaction R3 therefore makes the crucial contribution by increasing the abundance of OH which allows R20 to accelerate until the fuel is depleted..

Table 1: Reaction numbers and rate data for the principal elementary reactions in the hydrogen-air flame. These reactions are from GRI-Mech 3.0 [5] renumbered for the hydrogen-oxygen sub-mechanism.

number	reaction	A	b	E
R3	$\mathrm{O + H_2 \rightleftharpoons H + OH}$	$3.87 \cdot 10^4$	2.7	6260.0
R8	$\mathrm{H + O_2 + H_2O \rightleftharpoons HO_2 + H_2O}$	$1.13 \cdot 10^{19}$	−0.8	0.0
R9	$\mathrm{H + O_2 + N_2 \rightleftharpoons HO_2 + N_2}$	$2.60 \cdot 10^{19}$	−1.2	0.0
R10	$\mathrm{H + O_2 \rightleftharpoons O + OH}$	$2.65 \cdot 10^{16}$	−0.7	17041.0
R17	$\mathrm{H + HO_2 \rightleftharpoons 2\,OH}$	$8.40 \cdot 10^{13}$	0.0	635.0
R20	$\mathrm{OH + H_2 \rightleftharpoons H + H_2O}$	$2.16 \cdot 10^8$	1.5	3430.0

4 Premixed Methane Flame

Discussion of the premixed methane flame example will be included in the submitted paper and in the oral presentation.

5 Conclusion

Advances in computer power and in mathematical algorithms make it possible to perform detailed chemical simulations of flames economically with a minimum of simplifying models. New diagnostics will be needed to extract information from these simulations. Conversely, the manner in which diagnostics are applied to experiments may need to change to facilitate comparison of the simulation with experiment. For example, planar laser induced fluorescence (PLIF) images are routinely processed to account for loss of signal due to quenching of activated molecules. This correction depends on the abundance of quenching species which cannot be known a priori. An alternative approach is to apply quenching corrections to the simulation thereby permitting direct and unambiguous comparison of the simulation with raw signal data. This is currently possible for some species such as nitric oxide [21], but many other important diagnostic species such as OH remain to be examined.

Acknowledgments

This research was by the United States Department of Energy Office of Advanced Scientific Computing Research, Computational Science Research and Partnerships Division.

References

[1] C. F. Curtiss and J. O. Hirschfelder. *Proc. Natl. Acad. Sci. USA*, 38 (1952) 235–243.

[2] N. Peters and J. Warnatz, editors. *Numerical Methods in Laminar Flame Propagation*, Vol. 6 of *Notes on numerical fluid mechanics*. Vieweg-Verlag, Braunschweig, 1982. Proceedings of a GAMM workshop held at Aachen on October 12-14, 1981.

[3] R. J. Kee, J. F. Grcar, M. D. Smooke, and J. A. Miller. PREMIX: A fortran program for modeling steady, laminar, one-dimensional premixed flames. Technical Report SAND85-8240, Sandia National Laboratories, Livermore, 1983.

[4] I. Glassman. *Combustion*. Academic Press, third edition, 1996.

[5] G. P. Smith, D. M. Golden, M. Frenklach, N. W. Moriarty, B. Eiteneer, M. Goldenberg, C. T. Bowman, R. K. Hanson, S. Song, W. C. Gardiner Jr., V. V. Lissianski, and Z. Qin. GRI-Mech 3.0. Available from the world wide web: `http://www.me.berkeley.edu/gri_mech/`.

[6] M. J. Berger and P. Colella. *J. Comput. Phys.*, 82 (1989) 64–84.

[7] A. S. Almgren, J. B. Bell, P. Colella, L. H. Howell, and M. L. Welcome. *J. Comput. Phys.*, 142 (1998) 1–46.

[8] M. S. Day and J. B. Bell. *Combust. Theory Modelling*, 4 (2000) 535–556.

[9] J. B. Bell, N. J. Brown, M. S. Day, M. Frenklach, J. F. Grcar, and S. R. Tonse. *Proc. Combust. Inst.*, 28 (2000) 1933–1939.

[10] J. B. Bell, M. S. Day, I. G. Shepherd, M. Johnson, R. K. Cheng, J. F. Grcar, V. E. Beckner, and M. J. Lijewski. *Proc. Natl. Acad. Sci. USA*, 102 (2005) 10006–10011.

[11] J. B. Bell, M. S. Day, J. F. Grcar, M. J. Lijewski, J. F. Driscoll, and S. F. Filatyev. *Proc. Combust. Inst.*, (2006) in press.

[12] W. C. Gardiner, Jr. *The Journal of Computational Chemistry*, 81 (1977) 2367–2371.

[13] A. Chrissanthopoulos, G. Skevis, and E. Mastorakos. Analysis of methane-air flame structures near extinction limits using CSP. In *proceedings of the Fourth GRACM Congress on Computational Mechanics*, 2002. Patra, June 27–29.

[14] S. H. Lam and D. A. Goussis. *Proc. Comb. Inst.*, 22 (1988) pp. 931+.

[15] A. Massias, D. Diamantis, E. Masorakos, and D. A. Gousis. *Combustion and Flame*, 117 (1999) 685–708.

[16] J. B. Bell, M. S. Day, J. F. Grcar, and M. J. Lijewski. *J. Comput. Phys.*, 202 (2005) 262–280.

[17] J. B. Bell, M. S. Day, J. F. Grcar, and M. J. Lijewski. A computational study of equivalence ratio effects in turbulent, premixed methane-air flames. In *Proc. ECCOMAS-CFD*, 2006. In press.

[18] J. B. Bell, M. S. Day, J. F. Grcar, and M. J. Lijewski. *Communications in Applied Mathematics and Computational Science*, 1 (2006) 29–51.

[19] J. B. Bell, R. K. Cheng, M. S. Day, and I. G. Shepherd. *Proc. Combust. Inst.*, (2006) in press.

[20] J. F. Grcar, J. B. Bell, and M. S. Day. *Combust. Theory Modelling*, 10 (2006) 559–580.

[21] J. B. Bell, M. S. Day, J. F. Grcar, W. G. Bessler, C. Schultz, P. Glarborg, and A. D. Jensen. *Proc. Combust. Inst.*, 29 (2002) 2195–2202.